Evaluating the Effects of Border Zone Approximations with Subject Specific Ischemia Models

D.J. Swenson[1,3], J.G. Stinstra[1,2], B.M. Burton[1,3], K.K. Aras[1,3], L.J. Healy[3], and R.S. MacLeod[1,2,3]

[1] Scientific Computing and Imaging Institute, University of Utah, Salt Lake City, USA
[2] Nora Eccles Harrison Cardiovascular Research and Training Institute, University of Utah, Salt Lake City, USA
[3] Department of Bioengineering, University of Utah, Salt Lake City, USA

Abstract— **Current computational models of acute ischemia are deficient because of their inability to be validated against experimental data and their lack of geometric realism. Past models of ischemia have been based on geometric primitives or hearts for which no electrical measurements exist. One consequence is that it is necessary to make modeling assumptions that are not supported by measurements or direct validation with experiments. Based on our subject specific simulations and measurements, we hypothesize that assumptions about the nature and scale of the border zone play a significant role in determining the cardiac potential distributions from ischemic sources of injury current. Geometrically accurate models were created from Magnetic Resonance Imaging (MRI) and Diffuser Tensor Imaging (DTI) after an in situ canine ischemia experiment. The ischemic zone was defined based on transmural electrode readings and was used in a static bidomain simulation representing a time point during the ST segment. Varying the width of the border zone in the simulations changed the magnitude and distribution of epicardial depressions and elevations. We also found that a border zone with linear variation of potential from healthy to ischemic regions was not adequate to simulate measured potentials. A more sophisticated border zone that included an explicit region of partial ischemia was necessary to simulate the field gradients seen in experimental data.**

Keywords— **ischemia, bidomain, subject-specific, border zone**

I. INTRODUCTION

ST-segment elevation and depression in ECG signals are important indicators of myocardial ischemia, despite a incomplete understanding of their physiological mechanisms and clinical interpretations [1]. Simulations based on the bidomain approach to modeling electric potentials in myocardial tissue have been used to evaluate proposed mechanisms that give rise to the development of the depressions and elevations on the epicardial surface [7]. However, researchers and clinicians have been unable to draw strong correlations between the locations of the ST depressions and the location of the ischemic zone using either current clinical standards or bidomain models. Most reports have concluded that more sophistication is required in the models in order to better represent the distribution of epicardial potentials during ischemia [2,5].

Traditionally, these models consist of three distinct regions: the border zone, ischemic zone, and healthy myocardium and geometric approximations of these regions are thought to be a significant source of simulation error [3]. The ischemic region is traditionally modeled as a wedge or square shaped ischemic zone that begins at the subendocardium and extends transmurally toward the endocardium with an extent representative of the degree of ischemia [2,3,4,5]. The ischemic region is one continuous region with homogeneously depressed membrane potential. In such formulations, the border zone is a relatively narrow (3 mm or less) zone in which the membrane potential transitions smoothly from the ischemic to the healthy values.

We hypothesize that the details of the border zone play a significant role in determining the epicardial potential distributions. Typical models assume a binary state of ischemia and thus a sharp transition between two homogeneous regions [2,3,4,5], a formulation derived from studies of infarcted hearts in which there is a distinct, sharp but irregular boundary between healthy and necrotic muscle cells [8]. Acute ischemia, however, is a very dynamic and spatially heterogeneous process only incompletely understood [7]. Thus the shape and width of an ischemic border zone could vary significantly from those in infracted hearts. Because injury currents, the primary source of epicardial depressions, develop in the border zone, the shape of the border zone is likely to impact the surface potentials [3].

We have created subject specific models from ischemia experiments that allowed direct comparison with measurements. Rather than fixing the border zone, its parameters became adjustable parameters in the model that were varied to best match the measured epicardial potentials. Post mortem MRI and DTI scans provided the basis for geometric models and measurements of ST potentials from 450 transmural electrodes determined location of ischemic changes.

Using a model that only consisted of the three traditional regions: ischemic zone, border zone, and healthy tissue, it was not possible to reproduce measured epicardial potentials. To account for heterogeneity, we added an additional

region that represented a partially ischemic zone. The fully ischemic region transitioned smoothly to a larger, less ischemic region. A much sharper transition was then implemented between the partially ischemic region and the healthy tissue. This produced epicardial potential differences that were much closer to what was measured experimentally.

II. METHODS

A. Experimental Setup

Ischemia was induced in an open chest canine preparation by cannulating the LAD artery and controlling the flow of blood with a digital rotary pump routing the blood from one of the carotid arteries. The heart was paced from the atrial appendage using a pacing clip while the blood gasses were monitored and corrected using a respirator. A 247 electrode sock was placed around the heart and 45 fiberglass plunge electrode needles with 10 electrodes per needle were placed through the ventricles on the anterior of the heart. The data was collected using a 1024 channel recording unit at 1KHz sampling rate. After inserting the needles, 1 hour was given for the preparation related injury currents to subside. The flow rate was controlled at a rate of 23 ml/min, 16 ml/min, and 9 ml/min while the heart rate was reduced from 380 ms to 230 ms by increments of 30 ms for every flow rate. Every thirty seconds a recording was taken for 5-second increments and saved for later processing.

B. Geometric Model Creation

The excised heart was scanned with a 7 Tesla small animal scanner for an anatomical scan with approximately 450 micron resolution in all directions and a diffusion tensor imaging (DTI) scan to identify the fiber directions. Needle and sock electrodes were digitized and registered to correspondence points in the MRI scans. The software package Seg3D (software.sci.utah.edu) was used to segment heart tissue using classical segmentation techniques such as thresholding and watershedding algorithms. These segmentations were imported into the SCIRun simulation environment (software.sci.utah.edu) where Marching Cubes and Taubin's mesh fairing [10] algorithms were used to create smooth polygonal surfaces with up to 450,000 faces. Tetgen (tetgen.berlios.de) was then used to create the volume tetrahedral mesh of about 1.5 million elements. Subsequently, fiber directions were mapped to each element from the DTI data.

The shape of the ischemic zone was modeled based on the needle data. We choose a time instant in the middle of the ST segment and reconstructed the potential distribution within the myocardial wall. We used a volumetric Laplacian method to reconstruct the potential distribution throughout the volume based on 450 needle measurements. The ischemic border zone corresponded to an isosurface of the reconstructed potential distribution at an ischemic elevation of 11 mV.

C. Simulation

The simulation was based on a static bidomain approximation [4,6] described by equation (1).

$$\nabla \cdot \left(M_i + M_e \right) \nabla \phi_e = -\nabla \cdot M_i \nabla \phi_m \qquad (1)$$

Where M_i and M_e are tensors of the anisotropic conductivity and ϕ_e and ϕ_m are the extracellular and membrane potentials. The membrane potential is equal to the difference between the intracellular and the extracellular potentials. For ischemic regions, this difference was set at 30 mV in accordance with previous studies [4]. The relative ground was adjusted to match the measured voltages by integrating the potentials over both data sets and subtracting the difference. All simulations were implemented in the SCIRun problem-solving environment, which solves differential equation (1) using a finite element method [9]. The normalized conductivity values came from a computational evaluation of the published conductivity values by Stinstra et al [6].

Table 1 Bidomain normalized conductivity values

	Healthy	Ischemic
Intracellular longitudinal conductivity	1	1
Intracellular transverse conductivity	.05	.05
Extracellular longitudinal conductivity	1	.5
Extracellular transverse conductivity	.333	.25

The border zone was modeled by using a Gaussian blurring on the edges of the ischemic zone using equation (2)

$$G(t) = 30e^{\frac{-t^2}{2\sigma^2}} \qquad (2)$$

Where G(t) is the potential at the distance t from the ischemic zone and variance of the Gaussian distribution is the variable that controls the overall width of the border. This equation was used to evaluate the effects of border zone width.

The transition region was also modeled with a Gaussian function but with a much larger variance. The actual value of the variance was optimized to fit the data. When the

transition region was included in the model, the border zone started at the edge of the transition region and decreased to zero over a few millimeters as seen in Fig 1.
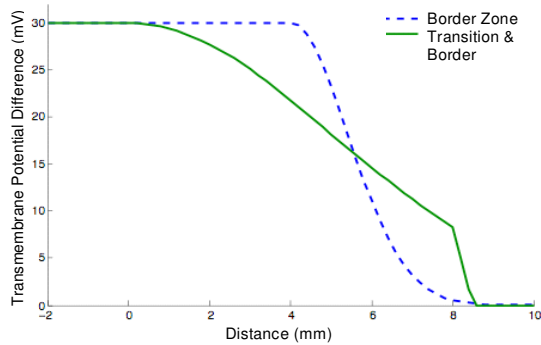

Fig. 1 Potential profile across border zone. The dashed blue line shows the transition from 30 mV transmembrane potential to 0 mV using a Gaussian function with a variance of 2. The green solid line shows a gradual transition region along with a sharp border zone.

III. Results

A. Approximation of the ischemic region

The elevated extracellular potentials in the center of the ischemic region transitioned smoothly to those in the healthy tissue—there was no evidence of two distinct regions. Fig. 2 shows the potentials from the needle data used to identify ischemic regions as an isosurface at 11 mV elevation over the baseline value. These surfaces represent the outer boundary of an ischemic region and inner surface of the surrounding border zone. When a transition zone was included in the model, the surface represented the interface between the ischemic and transition zones.
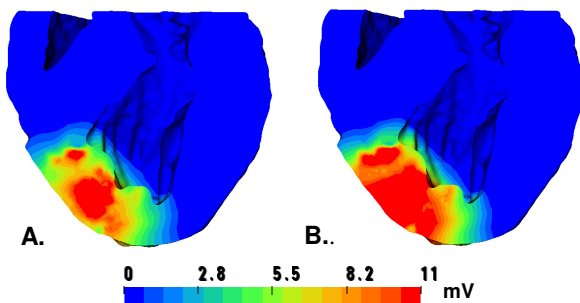

Fig. 2 A. An early stage of ischemia just becoming transmural. This corresponds to a run with a flow rate of 16 ml/min, paced at 320 ms. The scale was truncated at 11 mV to indicate the region considered ischemic in bright red. The maximum voltage was 18 mV. B. Shows a fully developed ischemia corresponding to a flow rate of 16 ml/min and paced at 230 ms. Maximum potential difference was 26 mV.

B. Border Zone Sensitivity

For a border zone with variance less than 2, the maximum elevation and minimum depression on the epicardial surface were highly sensitive to changes in the border zone. A variance of 2 corresponded to a border zone width of about 3 mm, which is commonly used in bidomain models. The resulting sharp transition produced depressions that were localized at the edges of the border zone. In contrast, the smoother transition of the border created depressions that were diffused across a larger area that was not specifically localized to lie over the border zone.
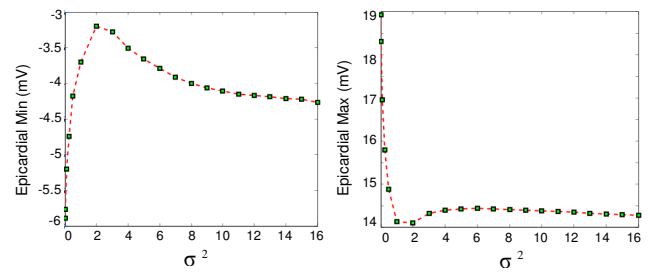

Fig. 3 ST-segment shifts as a function of border zone. The graph on the left shows the minimum epicardial potential in the simulation when the border was varied based on the given variance of a Gaussian distribution. The graph on the right is the corresponding maximum epicardial potential.

C. Matching the simulation with the experimental data

To simplify the results we divided the simulations into three groups, narrow border zones (less than 3 mm), wide border zones (10 mm to 15 mm), and simulations with transition regions. The narrow border zone simulations showed regions of steep epicardial potential gradients along their border separating homogeneous ischemic and healthy regions. This result was significantly different from the experimental data, which had field gradients within the ischemic region and in the healthy region. The gradients in the experimental data were much smaller in amplitude and more smoothly distributed than in the narrow border zone simulations. The wide border zones produced less severe gradients over the border zone, but also produced homogeneous epicardial potential elevations. The third set of simulations, that used a transition zone, resulted in field gradients that were closer in magnitude and distribution to the measured data. However, there were fewer gradients within the healthy region of the model. Figure [4 B] shows a simulation that included a transition region of 10 mm and a border zone of 3 mm.
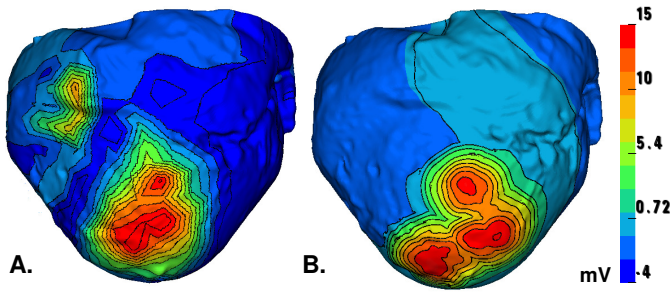
Fig. 4 Simulated and measured epicardial potentials during ischemia. Panel A shows measured extracellular potentials during the ST segment of an ischemia protocol. Panel B shows the simulated epicardial potentials from a subject specific model at a corresponding point in time.

IV. Discussion

A. Approximation of the ischemic region

The location, shape, and continuity of the ischemic zones reconstructed from the plunge needle electrodes, varied significantly from the ischemic zones seen in the literature [2,3,4,5]. Most simulations assume that the ischemic region is one continuous group of similarly ischemic cells, however, the data from this experiment did not support such an assumption. Results showed a small central region of maximum potential elevation that gradually transitioned to lower elevations. This gradual transition made it difficult to separate the border zone from the ischemic zone.

B. Border Zone Sensitivity

Varying the border zone width showed that the simulations where highly sensitive to rate of transition of membrane potential. Most simulations have failed to match the potential magnitudes seen in experimental data [2,7], a finding largely attributed to the anisotropy ratios chosen in the bidomain models. However, our results indicate that the border zone width and profile are important factors in determining the magnitude and shape of the elevations and depressions on the epicardial surface. Sharper border zone transition regions produced more localized and severe depressions, which occurred near features such as corners and parts of the border zone with high curvature. In fact, any feature in the potential distribution that produced a sharp transition had a significant effect on the potential distribution. This finding suggests a source of artifact in any simulations that use geometry with sharp corners, such as square ischemic zones, which are obviously not physiologically correct.

C. Matching the simulation with the experimental data

We were unable to match the epicardial potential distribution using the traditional model of a border zone regardless of border zone width. This finding, along with the absence of a distinct ischemic border in the measured needle electrode data, led us to create a transition region in the biodomain model. Inclusion of this transition region created epicardial field gradients similar to those seen in measurements. A much sharper transition was then implemented between the partially ischemic region and the healthy tissue, which was necessary to achieve distinct depressions located along the border zone.

It is apparent that the border zone is much more complex then previously thought and that it plays a significant role in the distribution and magnitude of the epicardial potentials. More research is needed to validate these findings and determine the actual shape of the transition region. More research is also needed to validate and explore the physiological significance of a transition region in ischemia.

REFERENCES

1. Wolferth C, Bettet S, Livezey M, et al. (1945) Negative displacement of the RS-T segment in the electrocardiogram and its relationships to positive displacement: An experimental study. Am Heart J 29:220
2. Kilpatrick D, Johnston P, Li D (2003) Mechanisms of ST change in partial thickness ischemia. J Electrocardiol 36 Suppl:7–12
3. Hopenfeld B, Stinstra J, Macleod R (2004) Mechanism for ST depression associated with contiguous subendocardial ischemia. J Cardiovas Electrophysiol 15:1200--1206
4. Hopenfeld B, Stinstra J, Macleod R (2005) The effect of conductivity on ST-segment epicardial potentials arising from subendocardial ischemia. Ann Biomed Eng 33:751-763
5. Johnston P, Kilpatrick D (2003) The effect of conductivity values on ST segment shift in subendocardial ischemia. IEEE Trans Biomed Eng 50:150—158
6. Stinstra J, Shome S, Hopenfeld B, MacLeod R (2005) Modelling passive cardiac conductivity during ischemia. Med Biol Eng Comput, 43776—782
7. Li D, Li CY, Yong AC, Kilpatrick D (1998) Source of electrocardiographic ST changes in subendocardial ischemia. Circ Res 82:957—970
8. Ursell P, Wit A, et al. (1985) Structural and electrophysiological changes in the epicardial border zone of canine myocardial infarcts during infarct healing. Circ Res 56:436--451
9. Sachse F, Stinstra J, et al. (2006) A software framework for solving bioelectrical field problems based on finite elements. Conf Proc IEEE Eng Med Biol Soc I:2554—2557
10. G. Taubin (1995) A signal processing approach to fair surface design. Conf Proc SIGGRAPH'95:351-358

Author: Darrell Swenson
Institute: Bioengineering Department, University of Utah
Street: 72 South Central Campus Drive
City: Salt Lake City
Country: USA
Email: darrell@sci.utah.edu